An experimental analysis of Lithium battery use for high power application.

Gabriele Bandini, *Gianluca* Caposciutti*, *Mirko* Marracci, *Alice* Buffi, and *Bernardo* Tellini

Department of Energy, Systems, Territory and Construction Engineering (DESTeC), University of Pisa, Italy

Abstract. In the recent years, the sustainable energy demand is growing among the civil and industrial sectors. However, the renewable sources present an aleatory behaviour, and the improvement of their reliable and secure employment have received great interest. In this framework, the energy storage devices can be used to smooth the market demand and to increase the control on the energy fluxes over transmission lines. To this aim, devices such as Li-ion batteries are widely used in several application scenarios, such as the transportation sector. Generally speaking, batteries are often classified as high-energy devices and their use for high-power applications is limited. Indeed, for the latter applications, other devices, such as supercapacitors or ultracapacitors, are usually employed. In the present work, the use of 3Ah 18650 Li-Ion batteries is investigated for high-power applications, and a performance analysis during pulsed discharge with current up to 50C is carried out. These experimental conditions are significantly beyond the manufacturer specifications; therefore, an accurate ageing estimation of the cell is required, and a novel internal resistance control method is proposed to monitor the state of health of the device.

1 Introduction

In the recent years, the use of sustainable energy sources is growing among civil and industrial sectors. Indeed, around 18% of the gross final energy consumption in Europe comes from renewables [1]. Among them, wind and solar energy have a significant share; however, they present an aleatory behaviour and the improvement of their reliable and secure use is of great interest. In this framework, the energy storage devices can be used to smooth the market demand and to increase the control on energy fluxes over transmission lines. To this aim, devices such as Li-ion batteries are widely employed in several application scenarios, such as the electric transportation sector. Usually, batteries are classified as energy-oriented devices and their use for high-power applications is limited. Therefore, other devices, such as supercapacitors or ultracapacitors, are preferably employed. Indeed , the use of high power batteries is made at expenses of battery state-of-health reduction, low performance and low energy density per unit of volume or of mass [2]. Recently, the study of pulsed power applications adopting lithium batteries is gaining interest. For instance, Shaoqing *et al.* [3] state that pulse charging has several benefits such as constructing stable solid electrolyte interface (SEI) film, speeding the charging rate, warming up the cold battery and possibly inhibiting the growth of lithium dendrites. Pulse discharge has been studied by Passerini *et al.* in [4], where a maximum current rate of 1.3C was employed during the tests on a 312 A Li-ion cell. They found the possibility to provide up to 800 cycles during pulse discharge, without occurring any safety issue. Huang *et al.* [5] study the pulsed charging-discharging process, and they find that it is possible to adopt pulses up to 3C with minor affection to the battery capacity decay over time by providing enough time to the voltage relaxation after the pulse. Particularly, the pulse-pause is used to mitigate the lithium ion migration to anode or cathode during the pulse, and hence the restraining of the side reactions by reducing the growth of SEI layer. The effect of higher rate discharge is studied by Wong *et al.* [6]. They employed a 15C rate profile on a LiFePO4 cell, finding that a growth of an internal high-impedance film due to the pulses is the main cause of the kinetics reduction of the charge transfer and storage processes. They also evaluate that the SEI film has a minor impact in the cell capacity fade effect. Recently, Marracci *et al.* [7] studied the effect on high discharge pulses, i.e. above 100C, on LiFePO4 cell 2.5 Ah, by adopting the test procedure defined in [8]. In particular, by using a classical model resistance parameter to manage the maximum pulse number for the single discharge, they reached 60000 pulses along the battery life.

In the present work, 3Ah LiNiMnCoO2 cells are studied and characterized under severe discharge pulse

* Corresponding author: gianluca.caposciutti@gmail.com

© The Authors, published by EDP Sciences. This is an open access article distributed under the terms of the Creative Commons Attribution License 4.0 (http://creativecommons.org/licenses/by/4.0/).

currents. By applying the pulse limitation criteria introduced by two of the authors [7], [8], 20C to 50C pulsed currents were imposed to the batteries. Being these experimental conditions significantly beyond the manufacturer specifications, an accurate ageing estimation of the cell has been carried out, and a novel internal resistance control method is proposed to monitor the state-of-health of the device.

The paper is organized as follows. In Section 2 the method is introduced, together with the description of the device under test, the experimental apparatus and the test conditions. In Section 3 the results are discussed by comparing performance obtained by different discharge rates, and by analyzing the device state-of-health. Finally, conclusions are drawn in Section 4.

2 Method

2.1 Device under test and pulse train stop condition

Within the present work, extreme discharge conditions are applied to the device under test (DUT) in order to estimate its performance in high power and low energy applications. The DUT is a LG18650 Lithium-ion battery cell, whose characteristics are briefly reported in Table 1.

Table 1. LG18650 HG2 technical specifications overview [9].

Type	$LiNiMnCoO_2$
Equivalent resistance	<20 mΩ (@ 1kHz)
Capacity (@std. rate)	3 Ah/10.8Wh
Nominal Voltage	3.6 V
Maximum Voltage (V_{max})	4.2 V
Minimum Voltage (V_{min})	2.5 V
Standard cycle conditions	I_{charge} = 1.5A $I_{discharge}$ = 0.6A
Maximum « fast » cycle conditions	I_{charge} = 4A $I_{discharge}$ = 4A $I_{discharge}$ = 20A(limit)

As shown in Table 1, the maximum discharge rate is approximatively 6.6C. In the course of the experiments, the DUT is tested at 20C, 30C, 40C and 50C rates (i.e. 60A, 90A, 120A and 150A current) pulsed discharge conditions. The determination of the stop criteria for the pulse train during a single pulsed discharge phase is critical in order to avoid a quick reduction of the cell capacity and of the State of Health (SoH). A single pulse discharge is made at constant current; hence, the electronic load imposes a voltage drop ΔV to the cell in order to obtain the desired discharge rate. According to this fact, the cell potential can reach lower values than minimum voltage V_{min} suggested by the manufacturer. The adoption of a minimum open circuit potential (OCP) criterion could be used as stop condition [8]. However, it can lead the cycle number per series to be much limited, with minor impact on the cell SoH as suggested by Marracci *et al.* [7].

Casals *et al.* [10] suggested that the cell internal resistance can be useful to assess the *SoH* of the device over the pulses, and also of the State of Charge (SoC) of the DUT. In the present work, we use a resistance parameter as end of pulse train parameter consistently with previous studies on batteries with different technologies [7]. The resistance parameter R_0 is then defined according to the Ohm's law as:

$$R_0 = \frac{\Delta V}{I_p} \quad (1)$$

According to the battery equivalent simple first order model, the R_0 is estimated around 20 mΩ as also reported by the manufacturer specification in Table 1. This value is expected to be reduced and further grow from its initial value along the pulsed discharge test [8], [7]. Therefore, the end of pulse train is set when the measured R_0 (Eq.1) grows above its initial value.

2.2 Experimental setup

In order to provide the desired pulse discharge, a EA-EL 9080-510 B electronic load [11] is used, while a EA-PSE 9200-140 power supply [12] is employed to charge the cells in standard conditions with CC-CV profile. A LEM IT 400-S Ultrastad current transducer [13] is employed to measure the current feedback signal, which value is acquired by means of a NI 9219 module on a NI 9174 chassis. The same module is also used to monitor the battery voltage, and cathode and anode temperatures for safety reasons by means of two RTD (Pt100 1/10 DIN) sensors.

During the experimental analysis, the cell is housed inside a climatic chamber to keep the environment temperature constant at 30 °C. The present setup can produce pulses mainly between 300 ms and 500 ms as maximum performance. This value is consistent, for instance, with the typical time for the charge of an inductive storage of an XRAM generator [14]. However, further studies can be performed with longer pulses. A Labview® software is built in order to measure cell voltage, current and temperature, to implement the stop condition for the experiment, and to continuously perform charge/discharge of the cell up to 80% of the initial capacitance. The latter condition defines the 0% of the SoH and the end of test condition [15]. The cell capacity is evaluated as:

$$C = \int_{\tau_s}^{\tau_e} I \, dt \quad (2)$$

where τ_s ans τ_e define the integration interval along a full "fast" charge or discharge. In the present study, the residual capacitance C/C_{max} is used for comparison purposes, while C is calculated during discharge cycles.

The cell cycling strategy consists in a full charge in CC-CV mode in "fast" conditions (i.e. 4A charge current). Furthermore, full pulsed discharge at the desired rate is performed until the end of pulse train condition is met. However, each 2 cycles the cell is fully

discharged in "fast" conditions (i.e. 4A discharge current) to measure its capacity *C*, and then fully charged in CC-CV mode in "fast" conditions to proceed with the battery cycling. Before the test, a 4 full cycles training phase (with standard conditions) have been performed on the new battery to stabilize the cell internal chemical reactions. The procedure is resumed in Fig. 1, while the experimental setup is shown in Fig. 2.

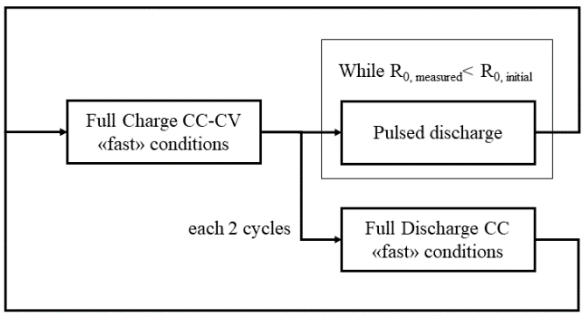

Fig. 1. Overview of the test procedure.

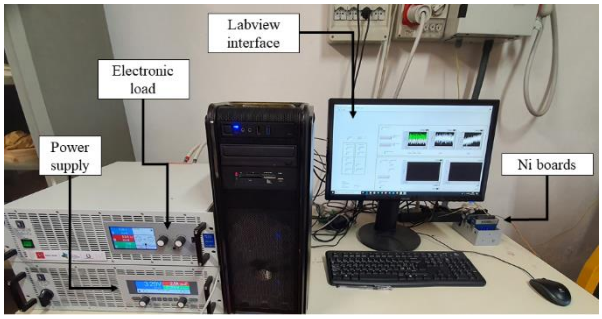

(a)

(b)

(c)

Fig. 2. (a) Overview of the test experimental apparatus, (b), the LG18650 HG2 and (c) the current measurement system LEM IT-400.

3 Results and discussion

3.1 General considerations

The typical behaviour of a single discharge pulse, and of a pulse train current-voltage profile over a full discharge cycle are presented in Fig. 3a, Fig. 3b and 3c, respectively.

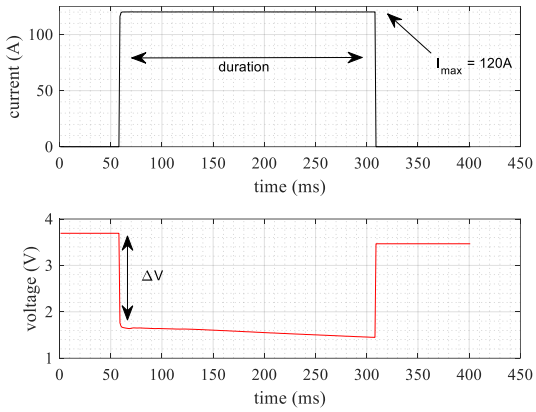

(a) 100th pulse of the series.

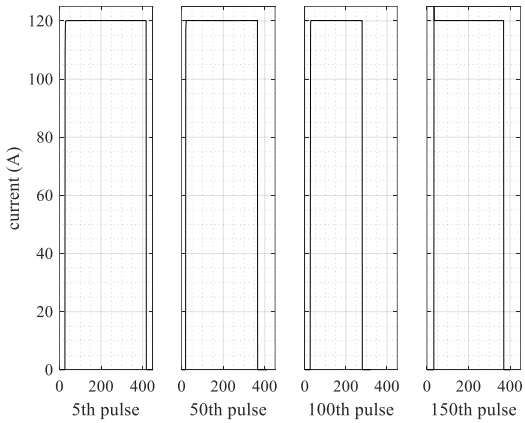

(b) Pulse train current as a function of the time (ms)

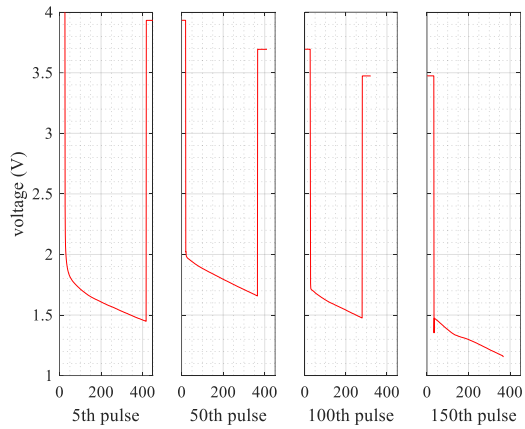

(c) Pulse train voltage as a function of the time (ms)

Fig. 3. Typical pulse behaviour at 40C discharge and 90% SoH.

As expected, the voltage drop leads the cell potential to reach values below the 2.5 V of minimum recommended voltage to ensure the desired discharge rate. It can be noticed by Fig.3c that the minimum voltage reached along the series is generally decreasing as a function of the pulse number. This is consistent with the energy deployment from the battery, which decreases also the initial pulse voltage. However, it is noteworthy that for the very first pulses a lower minimum cell potential can be reached. The first pulse starts after a full charge in standard condition, which contributes to redistribute the lithium ions over the cell. When the pulsed phase starts, a global accumulation of

the ion occurs according to Wong *et al.* [6], with chemical kinetic modification. This fact affects the cell performance (i.e. the discharge depth) only after a few pulses from the steady condition reached with the charge process. The latter consideration can also explain the behaviour of the R_0 during the pulse discharge phase, which is shown in Fig. 4.

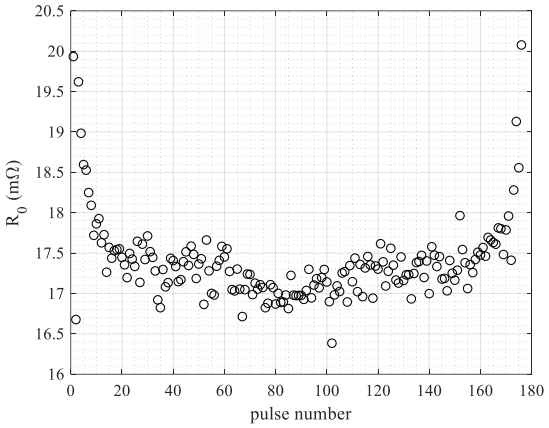

Fig. 4. Evolution of R_0 over a 40C pulse discharge series at 90% SoH.

Fig.4 shows that in the first part (pulse number < 20) the resistance parameter value decreases below the threshold limit of 20 mΩ until 17 mΩ. This fact is possibly induced by a transient regime affecting the internal chemical kinetics as aforementioned. A steady state operation is then maintained until a pulse number of 140. The low initial pulse voltage leads the system to be unable to maintain the set discharge current, thus reducing the provided current, and consequently increasing the R_0 value according to Eq.1. This also shows that the adopted threshold can consider the minimum energy of the cell to provide a discharge pulse.

3.2 Comparison between different discharge rate

The maximum number of cycles and cell performance reached during the tests at different discharge rate is resumed in Table 2.

Table 2. LG18650 HG2 performances at different pulse discharge rate.

Discharge rate	20C	30C	40C	50C
Discharge current	60A	90A	120A	150A
Total Cycles	52960	46017	19504	20
Median cycle number per discharge	348	227	172	na
Maximum cycle number per discharge	399	279	197	na

From the results shown in Table 2, the cell features allow a large amount of cycles at 20C and 30C, with 46000 to 52000 pulses on total, which is comparable with the results obtained by similar works operating with LiFePO4 nano phosphate cells, and a discharge rate well beyond the manufacturer specifications [7]. It is noteworthy that it is not possible to achieve a significant number of discharges when the current is above 150A (i.e. 50C). Moreover, this is not caused by cell temperature increase, since a maximum of 39 °C is obtained at the cell surface, but possibly an internal thermal damaging of cathode or anode due to Joule effect can occur during the pulses.

The energy discharged per pulse and the pulse duration distribution are showed in Fig. 5a and 5b, respectively.

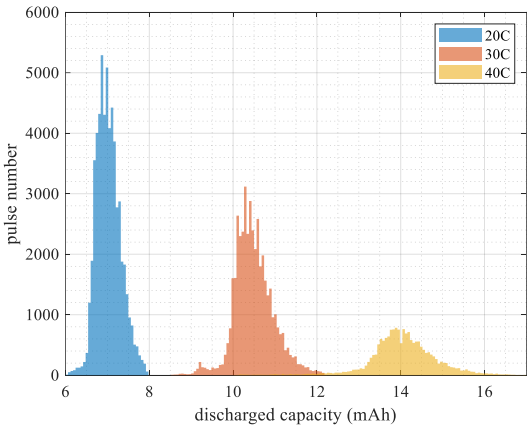

(a)

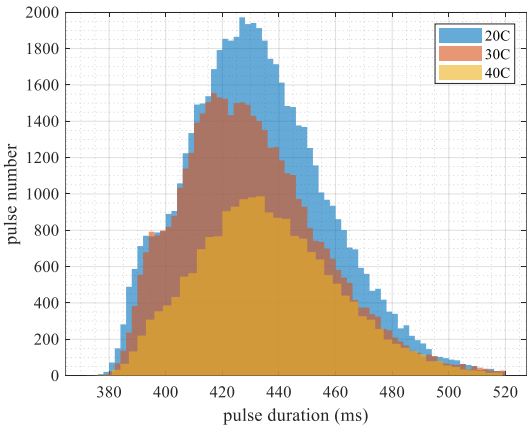

(b)

Fig. 5. Distribution of discharged capacity per pulse (a) and single pulse duration (b).

Table 3 shows an overview on pulsed discharge features.

Table 3. Pulse discharge features overview.

Discharge rate		20C	30C	40C
Discharged capacity (mAh)	med	7.0	10.4	14.0
	max	7.9	12.2	17.2
	min	6.0	8.6	10.1
Pulse duration	med	430.0	427.0	434.0
	max	519.0	518.0	519.0

(ms)	min	375.0	376.0	373.0

*med = median; min = minimum; max = maximum

As shown by Fig.5a and Table 3, a higher discharge rate leads to a higher discharged charge per pulse, as expected by the employed higher pulse current. However, especially at the end of the pulse train or at low SoH values, the cell residual potential does not allow to sustain a constant current pulse, thus reducing the released energy per pulse (see 150th pulse at low SoH value in Fig. 6). This also leads to increase the R_0 value above the threshold, possibly reaching the end of pulse train condition.

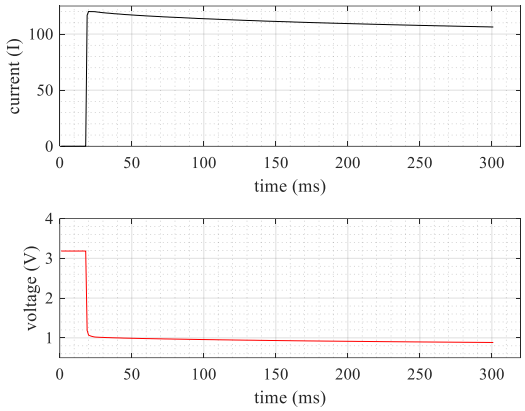

Fig. 6. Typical pulse behaviour at 40C discharge and 7% SoH, 150th pulse.

3.3 State of health analysis

The capacitance decay as a function of the pulse cycles is shown in Fig. 7a, while a standard capacity decay with 4A current cycles is shown in Fig. 7b for comparison purpose.

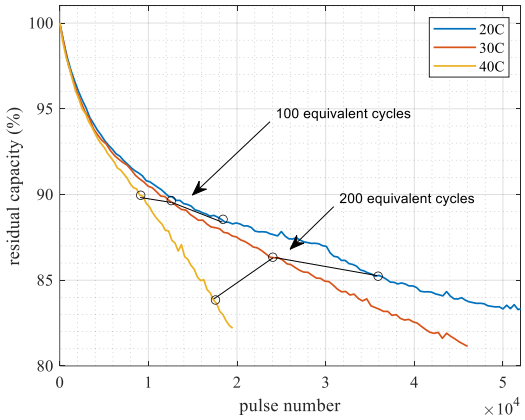

(a) Pulsed cycles

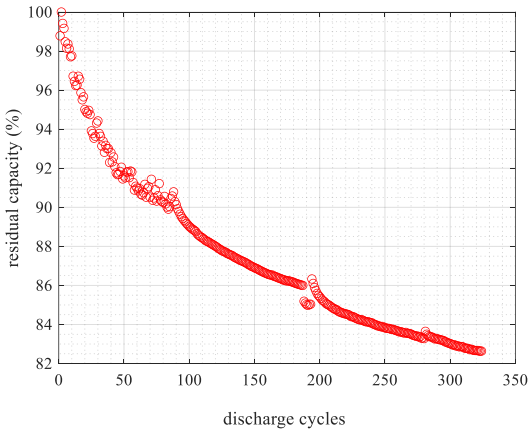

(b) Standard cycling

Fig. 7. Capacitance decay as a function of the pulse cycles

As expected, the capacitance decay for pulsed case is significantly faster when higher pulse current is applied. A first decay area (i.e. below 10k pulses) is found being not linear. The high decay rate leads the curves at different discharge current to be undistinguishable. Hereafter, a linear decay trend occurs with a slope which is proportional to the used discharge rate. The described behaviour is similar to the cell capacitance decay of a standard lithium battery presented in Fig 6b. However, at the same equivalent cycle number, the capacity decay is almost doubled during the whole life cycle of the DUT.

4 Conclusions

In the present work, pulsed current discharge conditions are adopted to test 3Ah lithium cells for high power applications. The employed currents are well beyond the limits imposed by manufacturer; however, the use of a novel State of Health-preserving strategy allowed to reach high performance and high pulses number. Particularly, more than 40k and 50k pulses have been achieved with 30C and 40C discharge rate, respectively. The maximum power discharged per pulse was around 200 W, and the capacity decay trend was observed being similar to a standard cycled cell. However, more than half of the life cycles was reached with pulse discharge conditions with respect to a standard cycle. The present findings showed that it is possible to deploy high power from small size lithium batteries with low state of health decay when a proper control criterion is applied, thus possibly converting Li-Ion batteries to competitive systems for high-power high-rate applications.

References

[1] Eurostat, Share of renewable energy in gross final energy consumption, (2020). https://ec.europa.eu/eurostat/databrowser/view/t2020_31/ (accessed July 18, 2020).

[2] P.H. Smith, R.B. Sepe, K.G. Waterman, L.J. Myron, Development and analysis of a lithium carbon monofluoride battery-lithium ion capacitor hybrid system for high pulse-power applications, J. Power Sources. 327 (2016) 495–506. https://doi.org/https://doi.org/10.1016/j.jpowsour.2016.07.035.

[3] S. Zhu, C. Hu, Y. Xu, Y. Jin, J. Shui, Performance improvement of lithium-ion battery by pulse current, J. Energy Chem. 46 (2020) 208–214. https://doi.org/https://doi.org/10.1016/j.jechem.2019.11.007.

[4] S. Passerini, F. Coustier, B.B. Owens, Lithium-ion batteries for hearing aid applications: II. Pulse discharge and safety tests, J. Power Sources. 90 (2000) 144–152. https://doi.org/https://doi.org/10.1016/S0378-7753(00)00396-7.

[5] H. Lv, X. Huang, Y. Liu, Analysis on pulse charging–discharging strategies for improving capacity retention rates of lithium-ion batteries, Ionics (Kiel). 26 (2020) 1749–1770. https://doi.org/10.1007/s11581-019-03404-8.

[6] D.N. Wong, D.A. Wetz, A.M. Mansour, J.M. Heinzel, The influence of high C rate pulsed discharge on lithium-ion battery cell degradation, in: 2015 IEEE Pulsed Power Conf., 2015: pp. 1–6. https://doi.org/10.1109/PPC.2015.7297030.

[7] M. Marracci, B. Tellini, Ageing Characterization of Li - Ion Batteries Discharged at High Pulse Current Rates, in: 2018 IEEE 4th Int. Forum Res. Technol. Soc. Ind., 2018: pp. 1–5. https://doi.org/10.1109/RTSI.2018.8548383.

[8] M. Marracci, B. Tellini, O. Liebfried, V. Brommer, Experimental tests for Lithium batteries discharged by high power pulses, in: 2015 IEEE Int. Instrum. Meas. Technol. Conf. Proc., 2015: pp. 1063–1067. https://doi.org/10.1109/I2MTC.2015.7151418.

[9] LG-Chem, Product specification. Rechargeable Lithium Ion Battery Model : INR18650HG2 3000mAh, 2014. https://cdn.shopify.com/s/files/1/0674/3651/files/lg-hg2-spec-sheet.pdf.

[10] L.C. Casals, A.M.S. González, B.A. García, J. Llorca, PHEV Battery Aging Study Using Voltage Recovery and Internal Resistance From Onboard Data, IEEE Trans. Veh. Technol. 65 (2016) 4209–4216. https://doi.org/10.1109/TVT.2015.2459760.

[11] Elektroautomatik, Electronic Load, (2019). http://www.farnell.com/datasheets/2057601.pdf?_ga=2.120352328.1300505852.1576835493-893386533.1576835493 (accessed December 20, 2019).

[12] Elektroautomatik, Power supply, (2019). https://elektroautomatik.com/media/pdf/54/6c/b2/06230700_EN.pdf (accessed December 20, 2019).

[13] Ultrastad, LEM IT 400-S, (2019). https://www.newtons4th.com/wp-content/uploads/2014/07/LEM-IT-400-S.pdf (accessed December 20, 2019).

[14] O. Liebfried, V. Brommer, A Four-Stage XRAM Generator as Inductive Pulsed Power Supply for a Small-Caliber Railgun, IEEE Trans. Plasma Sci. 41 (2013) 2805–2809. https://doi.org/10.1109/TPS.2013.2257873.

[15] S.F. Schuster, T. Bach, E. Fleder, J. Müller, M. Brand, G. Sextl, A. Jossen, Nonlinear aging characteristics of lithium-ion cells under different operational conditions, J. Energy Storage. 1 (2015) 44–53. https://doi.org/10.1016/J.EST.2015.05.003.